IET Optoelectronics

Research Article

IET Journals
The Institution of Engineering and Technology

Secured relay-assisted atmospheric optical code-division multiple-access systems over turbulence channels

ISSN 1751-8768
Received on 5th November 2014
Revised on 23rd April 2015
Accepted on 19th June 2015
doi: 10.1049/iet-opt.2014.0148
www.ietdl.org

Hien T.T. Pham[1] ✉, Phuc V. Trinh[2], Ngoc T. Dang[3], Anh T. Pham[4]

[1]*Department of Optical Communications, Posts and Telecommunications Institute of Technology, Km 10, Nguyen Trai Road, Ha Don District, Hanoi 100000, Vietnam*
[2]*Computer and Information Systems, University of Aizu, B 11-4, Tsuruga, Ikkimachi, Aizu-Wakamatsu, Fukushima 965-8580, Japan*
[3]*Department of Optical Communications, Posts and Telecommunications Institute of Technology, Km 10, Nguyen Trai Road, Ha Dong District, Hanoi, Hanoi 150000, Vietnam*
[4]*Computer Engineering, The University of Aizu, Tsuruga, Ikkimachi, Aizu-Wakamatsu, Fukushima 965-8580, Japan*
✉ *E-mail: hienptt@ptit.edu.vn*

Abstract: The authors propose a relay-assisted atmospheric optical code-division multiple-access (AO/CDMA) system for secured, multiuser optical communications. Chip detect-and-forward (CDF) scheme is used at relay nodes so that the complex multiuser decoding process can be avoided. The proposed system performance, in terms of bit-error rate (BER) and transmission confidentiality, is analysed over atmospheric turbulence channel taking into account channel loss due to atmospheric attenuation and beam divergence. Multiple-access interference and background noise are also included in the analysis. In addition, a quantitative analysis of data confidentiality is further examined in the study. The numerical results show that the relay transmission is an efficient solution to improve the system performance. Thanks to this solution, AO/CDMA systems can achieve low BER, long distance, and a large number of users. Moreover, high confidentiality can be attained by properly configuring system parameters, such as limiting the transmitted power and/or reducing the signal beam width.

1 Introduction

Atmospheric optical (AO) or free-space optical (FSO) communication, a data transmission technology based on the propagation of light over atmospheric channel, has recently received much attention thanks to its advantages of high data rates, unregulated spectrum, and flexible deployment [1]. Since AO communication is capable of providing Gigabits per second (Gbps) data rates, it is a promising candidate for broadband access environments [2]. To allow multiple users to simultaneously share the same resource of atmospheric channels, AO/code-division multiple-access (AO/CDMA) systems have been proposed and attracted much interest thanks to additional benefits including asynchronous access, scalability, and inherent security [3–8].

It has been shown in the literature that the performance of AO/CDMA systems is severely limited by the effect of atmospheric turbulence, which is caused by the variations in the refractive index due to inhomogeneities in temperature and pressure changes [9]. Atmospheric turbulence, together with background noise and multiple-access interference (MAI), causes the increase of bit-error rate (BER) and significantly limits the transmission distance of AO/CDMA systems. Several techniques have been proposed to deal with this problem, including pulse-position modulation (PPM), spectral phase encoding, and forward error correction (FEC). PPM offers a number of advantages, including power-efficient and non-threshold detection [3–7]. PPM-based AO/CDMA system, which requires the transmission of short pulse, is however significantly affected by pulse broadening effect in the case of transmitting high data-rate and long distance [8]. Spectral phase-encoded optical CDMA also offers better spectral efficiency and performance [6]. It is, nevertheless, relatively complicated since the use of coherent sources is required. The study in [7] shows that FEC can effectively combat with physical layer impairments. The use of FEC is still limited as it imposes high delay and reduces the transmission efficiency.

In this paper, we propose to use relay-assisted transmission to deal with atmospheric turbulence issue in AO/CDMA systems. Relay transmission is an effective technique to improve the coverage and reliability of radio frequency links, and it has been recently proposed in FSO communications [10–15]. By employing relay transmission, the performance and coverage distance of AO/CDMA systems can be improved. It also helps to deploy the system when users and the receiver do not have a line-of-sight connection. Conventional relay schemes often use bit detect-and-forward (BDF) at relay nodes [10, 11]. Nevertheless, BDF is complex in relay-assisted AO/CDMA systems since multiuser detection at each relay node is required. We therefore propose to use chip detect-and-forward (CDF) instead. In relay-assisted AO/CDMA systems using CDF scheme, relay nodes will detect CDMA chip, either '1' or '0', using a threshold detection, and then forward that chip to the following node. Furthermore, CDF can be well matched to AND detection scheme, which is used at the receiver to mitigate the effect of MAI [16].

In addition, although enhanced security has been often cited as an advantage of both AO communication and optical CDMA, the quality and degree of security enhancements have not been examined for AO/CDMA systems. As a matter of fact, it is possible for someone to intercept a signal by placing a detector within the footprint of the optical beam, especially when the beam width is wider due to the long transmission distance. In this paper, we also consider the code interception performance of the proposed AO/CDMA systems, which is calculated based on the probability that the eavesdropper can detect the user's entire code word with no errors.

In our analysis, the performance of relay-assisted AO/CDMA systems over atmospheric turbulence modelled as log-normal fading channel will be carried out taking into account major physical layer impairments including MAI and background noise. Other effects of atmospheric channel such as atmospheric attenuation and power loss due to beam spreading are also considered. The expression for BER and transmission

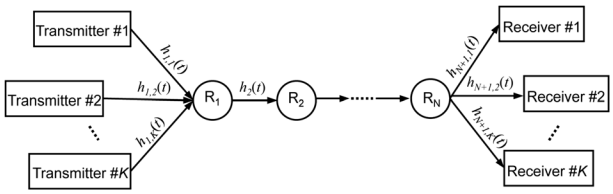

Fig. 1 *Relay-assisted AO/CDMA system model*

confidentiality of the proposed AO/CDMA systems will be analytically derived. Numerical results will be discussed considering various system's parameters, including the transmitted power, the number of relays, the number of users, and the transmission distance.

The rest of the paper is organised as follows. The model of relay-assisted AO/CDMA systems is introduced in Section 2. Section 3 presents the mathematical model of atmospheric channel. In Section 4, we formulate the BER of relay-assisted AO/CDMA systems. Section 5 devotes to analyse the security performance of the proposed system. The numerical results and discussion are shown in Section 6. Finally, Section 7 concludes the paper.

2 Relay-assisted AO/CDMA System

2.1 System model

A model of a relay-assisted AO/CDMA system with K users and N relays is shown in Fig. 1. Data signals from all K users are transmitted over atmospheric channels and collected by the first relay (R_1), where they are detected and then forwarded to the receiver via other relays (i.e. R_2, R_3,…, R_N). Each user in the AO/CDMA system is assigned a unique signature code, which can be either one-dimensional or two-dimensional (2D) one, for encoding its data. With the properties of high cardinality and low peak cross-correlation, 2D wavelength hopping/time spreading (WH/TS) codes have been proposed and adopted in optical CDMA systems [17]. To reduce MAI and enhance security, 2D WH/TS codes are also used in our proposed AO/CDMA system, whose block diagram, including a transmitter, a relay, and a receiver, is depicted in Fig. 2.

At the transmitter side shown in Fig. 2*a*, binary data of each user is first modulated with broadband optical signal, which is generated from the laser source, at a modulator. Modulated optical signal is then encoded in both wavelength and time domains at a WH/TS encoder, where bit '1' is converted to a chip sequence including chips '1' and '0' while bit '0' is kept unchanged. An optical pulse at a specific wavelength, whose power is P_c, will be transmitted in the case of chip '1' while optical pulse is absent in the case of chip '0'.

At the first relay, as shown in Fig. 2*b*, optical pulses from K users are collected and separated into individual wavelengths at a demultiplexer (λ-DEMUX). The optical signal at each wavelength is then converted to an electrical signal by a photodetector (PD). The electrical signal is then followed a process of CDF by a threshold detector and a laser source. Optical signals from laser sources are combined at a wavelength multiplexer (λ-MUX) before transmitting to the next node. It is worth noting that the transmitted power per chip '1' at the output of R_1 is also kept at the level of P_c. The similar process is performed at other relays (i.e. R_2, R_3, …, R_N) of the system. The CDF process in these relays is not affected by additional MAI as they are only connected to the previous node.

At the receiver (Fig. 2*c*), the binary data from the desired transmitter is decoded at a WH/TS decoder. After passing through the decoder, optical pulses (i.e. chip '1'), whose wavelengths are matched to receiver's signature codes, are collected and separated. In addition, the relative time delays among them are cancelled so that they are aligned in time. Next, these optical pulses are converted to electrical ones at the PDs and then detected at chip detectors. Based on logical levels at the output of the chip detectors, logical AND operation is carried out to detect a bit '1' or a bit '0'.

2.2 Prime code

In this paper, we use 2D prime code to provide accessibility for multiple users simultaneously. In detail, each user is assigned a unique code whose length is p_s^2, where p_s is a prime number. A TS pattern can be generated using the linear congruent placement operator to place a pulse within a block as follows

$$c_{xy} = [x.y] \quad x, y = 0, 1, \ldots, p_s - 1, \tag{1}$$

where [.] denotes modulo p_s operation, x represents the sequence number within the family of sequences, and y represents the block number for that particular sequence. The algorithm determines the place of a pulse within a block of length p_s. Hence, the prime algorithm produces p_s sequences ($i = 0, 1, \ldots, p_s - 1$) of length p_s^2.

Similarly, a WH pattern is generated from a prime number p_h ($p_s \leq p_h$). In that case, there are p_h wavelengths available for colouring the TS pattern, exactly as there are p_s pulses in the code sequence. The WH pattern H_0 comprises pulses at one wavelength only and is therefore discarded. Consequently, the number of WH patterns is $p_h - 1$ and a 2D WH/TS code set includes $p_s \times (p_h - 1)$ distinctive 2D prime codes of length p_s^2. The process of generating the TS and the WH patterns with $p_s = p_h = 5$ is illustrated in Table 1. An example of 2D WH/TS code sequence created by WH pattern H_1 and TS pattern S_2 is $\lambda_0 000\ 000 \lambda_1 000\ \ 000 \lambda_2\ 0 \lambda_3 000\ 000 \lambda_4 0$.

3 Atmospheric channel

Considering the effects of path loss and atmospheric turbulence, the state of atmospheric channel between node ($m - 1$) and node m can

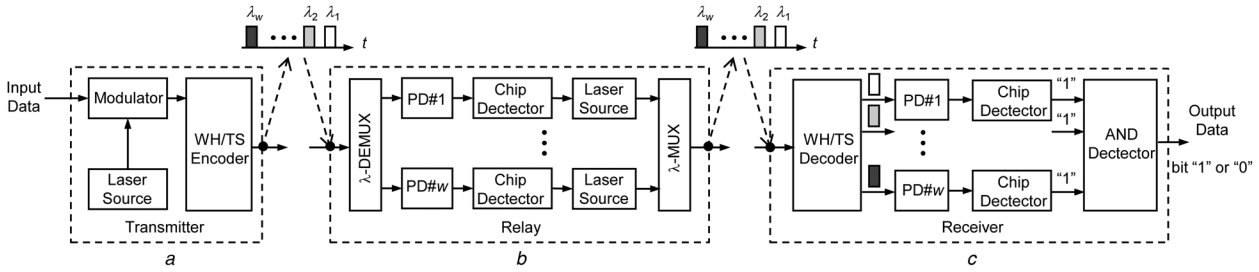

Fig. 2 *Block diagram of*

a Transmitter
b Relay node
c Receiver in relay-assisted AO/CDMA system

Table 1 WH and TS patterns for $p_s = p_h = 5$

WH pattern	TS pattern
H_0 $\lambda_0\lambda_0\lambda_0\lambda_0\lambda_0$	S_0 10000 10000 10000 10000 10000
H_1 $\lambda_0\lambda_1\lambda_2\lambda_3\lambda_4$	S_1 10000 01000 00100 00010 00001
H_2 $\lambda_0\lambda_2\lambda_4\lambda_1\lambda_3$	S_2 10000 00100 00001 01000 00010
H_3 $\lambda_0\lambda_3\lambda_1\lambda_4\lambda_2$	S_3 10000 00010 01000 00001 00100
H_4 $\lambda_0\lambda_4\lambda_3\lambda_2\lambda_1$	S_4 10000 00001 00010 00100 01000

be described as

$$h_m = h_m^{\mathrm{l}} h_m^{\mathrm{p}} h_m^a, \tag{2}$$

where h_m^{l} is the path loss coefficient, which is considered as a fixed scaling factor during a long period of time, h_m^{p} is the fraction of power collected by a PD, which depends on the relative distance (r) between the PD and the centre of the received optical beam, h_m^a is a random variable representing the intensity fluctuation due to atmospheric turbulence.

3.1 Channel loss

Channel loss is the reduction of the optical signal power as a result of absorption and scattering processes due to the presence of molecules along the transmission path. The concentrations of matter in the atmosphere, which depend on the weather conditions, result in the signal attenuation varying spatially and temporally. The attenuation of optical power through the atmospheric is described by the exponential Beers–Lambert Law and can be described as

$$h_m^{\mathrm{l}} = \exp(-\beta z), \tag{3}$$

where β is the attenuation coefficient and z is the transmission distance between node $(m-1)$ and node m, respectively.

3.2 Fraction of collected power

To compute the fraction of collected power by a desired user and an eavesdropper, we consider a circular detection aperture of radius a and a Gaussian beam profile at the receiver as shown in Fig. 3. For a Gaussian beam, the normalised spatial distribution of the transmitted intensity at distance z from the transmitter is given by

$$I_{\mathrm{beam}}(\rho; z) = \frac{2}{\pi\omega_z^2}\exp\left(-\frac{2\|\rho\|^2}{\omega_z^2}\right), \tag{4}$$

where ρ is the radial vector from the beam centre, and ω_z is the beam waist (radial calculated at e^{-2}) at distance z [18]. The loss due to geometric spreading with pointing error r (i.e. relative distance between the PD and the centre of the received optical beam) is

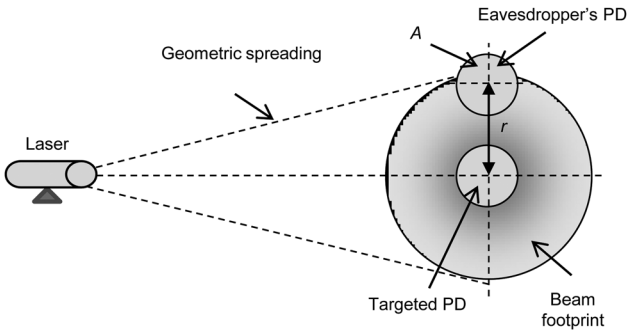

Fig. 3 *Location of PDs and beam footprint on the detector plane at the distance of z*

expressed as

$$h_m^{\mathrm{p}}(r; z) = \int_A I_{\mathrm{beam}}(\rho - r; z), \tag{5}$$

where A is the detector area. Equation (5) can be approximated by the Gaussian form as [19]

$$h_{\mathrm{p}}(r; z) = A_0 \exp\left(-\frac{2r^2}{\omega_z^2}\right), \tag{6}$$

where $\upsilon = \left(\sqrt{\pi}a\right)/\left(\sqrt{2}\omega_{\mathrm{zeq}}\right)$, and [19]

$$A_0 = [\mathrm{erf}(\upsilon)]^2, \quad \omega_{\mathrm{zeq}}^2 = \omega_z^2 \frac{\sqrt{\pi}\mathrm{erf}(\upsilon)}{2\upsilon\exp\left(-\upsilon^2\right)}. \tag{7}$$

Here, A_0 is the fraction of the collected power at $r = 0$, and ω_{zeq} is the equivalent beam width. It is worth noting that the fraction of collected power by the desired user can be calculated with $r = 0$.

3.3 Atmospheric turbulence

Transmission over free-space channel, whose refractive index and atmospheric temperature are fluctuated, results in signal fading commonly named as atmospheric turbulence. In AO/CDMA systems, this effect is the main factor that causes the degradation of signal quality and BER.

The atmospheric turbulence is also difficult to model because of erratic elements of atmosphere such as temperature, pressure and index. However, thanks to the statistical methods, there are a number of proposed mathematical models which can approximate this effect such as log-normal, gamma, gamma–gamma distributions. Each model corresponds to a specific range of turbulence strength. This paper deals with weak turbulent condition, thus the suitable model is log-normal distribution.

The log-normal random variable h_m^a can be found if we take the exponent of a normally distributed random variable X. Therefore, the relation between the optical signal intensity at the output of transmitter I_{T} and the optical signal intensity at the input of receiver I_{R} through atmospheric turbulent channel can be shown as

$$h_m^a = \frac{I_{\mathrm{R}}}{I_{\mathrm{T}}} = \mathrm{e}^X, \tag{8}$$

where X is the normally distributed random variable with mean μ_x and standard deviation σ_x. Its probability density function (pdf) can be described as

$$\Omega\left(X, \mu_x, \sigma_x^2\right) = \frac{1}{\sqrt{2\pi\sigma_x^2}}\exp\left(-\frac{X - {\mu_x}^2}{2\sigma_x^2}\right). \tag{9}$$

To fairly measure the fading effect caused by atmospheric turbulence, the mean of the log-normal random variable needs to be normalised to guarantee that the average received power is not attenuated or amplified by turbulence. Therefore, $\mu_x = -\sigma_x^2/2$ and the pdf of the log-normal variable can be expressed as

$$f_{\mathrm{P}}\left(h_m^a\right) = \frac{1}{h_m^a\sqrt{2\pi\sigma_x^2}}\exp\left(-\frac{\left[\ln\left(h_m^a\right) + (1/2)\sigma_x^2\right]^2}{2\sigma_x^2}\right), \tag{10}$$

and for weak turbulence, the variance of log-amplitude fluctuation σ_x^2 for spherical waves is given by [20]

$$\sigma_x^2 = 0.496\left(\frac{2\pi}{\lambda}\right)^{7/6} z^{11/6} C_n^2, \tag{11}$$

where λ and z are the wavelength and transmission distance in meters; C_n^2 is the refractive index structure coefficient.

4 Performance analysis

4.1 Bit error rate

In this subsection, the proposed system BER is analytically derived. Among K users, one user is assumed to be the desired user while $K-1$ remaining ones are probable interfering users. The total BER is conditioned on the events: k users among the $(K-1)$ probable interfering users may transmit a data bit '1', which follows a binomial distribution. Under the assumption that the probabilities of transmitting bit '1' and bit '0' are equally likely for all users, the BER at the receiver can be calculated as

$$\mathrm{BER} = \sum_{k=1}^{K-1} \left\{ \binom{K-1}{k} 2^{1-K} \cdot \frac{1}{2} \left[p_{\mathrm{be}}(0|1,\, k) + p_{\mathrm{be}}(1|0,\, k) \right] \right\}, \tag{12}$$

where $p_{\mathrm{be}}(0|1,\ k)$ and $p_{\mathrm{be}}(1|0,\ k)$ are the conditional bit error probabilities when detecting bit '1' and bit '0' at the receiver, respectively. In the case of AND detection shown in Fig. 2, logical AND operation is carried out on all '1' chip positions of the desired code to detect a bit '1' [16]. Conditional bit error probabilities therefore can be expressed in terms of the conditional chip error probabilities (CEPs) and for AND detection as

$$\begin{aligned} p_{\mathrm{be}}(0|1,\, k) &= \sum_{j=1}^{p_{\mathrm{s}}} \binom{p_{\mathrm{s}}}{j} [p_{e2e}(0|1,\, k)]^{j} [1 - p_{e2e}(0|1,\, k)]^{p_{\mathrm{s}}-j}, \\ p_{\mathrm{be}}(1|0,\, k) &= \prod_{j=1}^{p_{\mathrm{s}}} p_{e2e}(1|0,\, k), \end{aligned} \tag{13}$$

where $p_{e2e}(0|1,\ k)$ and $p_{e2e}(1|0,\ k)$ are end-to-end CEPs when the desired user transmits chip '1' but detects chip '0' and transmits chip '0' but detects chip '1'. It is clear that these probabilities depend on the CEPs of all hops from the desired transmitter to the receiver.

4.2 CEP for the first hop

CEP for the first hop is determined at the first relay (R_1). At the first hop, CEP is affected by not only background noise but also MAI from interfering users. We assume that the transmitted power per pulse (P_{c}) and the distance to R_1 are identical for both the desired user and $(K-1)$ remaining users. In addition, among the k users transmitting bit '1', n interfering users may have a pulse overlapping the chip of interest, where $n = \mathrm{binom}(k,\, p_{\mathrm{cov}})$ and p_{cov} is the probability that desired user's chip is overlapped by an interfering user's chip. For the case of 2D WH/TS prime code, $p_{\mathrm{cov}} = \mu_\lambda / p_{\mathrm{s}}^3$ [16], where μ_λ is the average number of wavelengths common to a pair of two codes and, under the condition that $p_h > p_{\mathrm{s}}$, can be estimated as [17]

$$\mu_\lambda = \frac{1}{\binom{p_h}{p_{\mathrm{s}}}} \left\{ \begin{aligned} &\binom{p_h-1}{p_{\mathrm{s}}-1} \frac{(p_h-1)(p_{\mathrm{s}}-2)+(p_h+2)}{p_h-2} \\ &+ \binom{p_h-1}{p_{\mathrm{s}}} \frac{p_{\mathrm{s}}(p_h-1)}{p_h-2} \end{aligned} \right\}. \tag{14}$$

In the special case that $p_h = p_{\mathrm{s}}$, μ_λ equals to p_{s}, therefore $p_{\mathrm{cov}} = 1/p_{\mathrm{s}}^2$.

Given k users transmitting bit '1', n can vary from 1 to k, therefore CEPs for the first hop can be computed as

$$p_{\mathrm{ce}-1}(1|0,\, k) = \sum_{n=1}^{k} \left\{ \binom{k}{n} p_{\mathrm{cov}}^{n} (1 - p_{\mathrm{cov}})^{k-n} p_{\mathrm{ce}}(1|0,\, n) \right\}, \tag{15}$$

$$p_{\mathrm{ce}-1}(0|1,\, k) = \sum_{n=1}^{k} \left\{ \binom{k}{n} p_{\mathrm{cov}}^{n} (1 - p_{\mathrm{cov}})^{k-n} p_{\mathrm{ce}}(0|1,\, n) \right\}, \tag{16}$$

where $p_{\mathrm{ce}}(1|0,\ n)$ and $p_{\mathrm{ce}}(0|1,\ n)$ are the conditional CEPs when detecting chip '1' and chip '0', respectively.

The conditional CEPs are governed by the received power per chip at the input of the relay R_1, which can be expressed as

$$P_{1(0)} = \sum_{i=1}^{n} h_{1,i} P_{\mathrm{c}} + P_{\mathrm{b}} = h_{1(0)} P_{\mathrm{c}} + P_{\mathrm{b}}, \tag{17}$$

$$P_{1(1)} = h_{1,\mathrm{d}} P_{\mathrm{c}} + \sum_{i=1}^{n} h_{1,i} P_{\mathrm{c}} + P_{\mathrm{b}} = h_{1(1)} P_{\mathrm{c}} + P_{\mathrm{b}}, \tag{18}$$

where $P_{1(0)}$ and $P_{1(1)}$ are the received optical powers when desired user transmits chip '0' and chip '1', respectively. P_{b} is the average background power. $h_{1,i}$ denotes the atmospheric channel coefficient of the ith interfering user and we assume that it has the same pdf with the desired one's (i.e. $h_{1,\mathrm{d}}$). Here, the sums of n or $(n+1)$ log-normal random variables can be approximated into a single log-normal random variable denoted as $h_{1(0)}$ or $h_{1(1)}$ (the detail about this approximation is given by (36) in Appendix 1).

When received optical signals pass through the PD, they are converted to the electrical currents which can be expressed as

$$I_{1(0)} = \Re h_{1(0)} P_{\mathrm{c}}, \tag{19}$$

$$I_{1(1)} = \Re h_{1(1)} P_{\mathrm{c}}, \tag{20}$$

where $I_{1(0)}$ and $I_{1(1)}$ are electrical signals respectively converted from $P_{1(0)}$ and $P_{1(1)}$ thanks to the PD. Besides, background power causes the background noise, whose variance can be written as

$$\sigma_{\mathrm{b}}^2 = 2e\Re P_{\mathrm{b}} B_{\mathrm{e}}, \tag{21}$$

where B_{e} corresponds to the effective electrical bandwidth.

Based on (19)–(21), the CEPs under the effects of MAI and background noise can be calculated as

$$\begin{aligned} &p_{\mathrm{ce}}(1|0,\, n) \\ &= \int_0^{\infty} \int_{I_{\mathrm{D}}}^{\infty} f_{\mathrm{P}}\left(h_{1(0)}^{a}\right) \frac{1}{\sqrt{2\pi\sigma_{\mathrm{b}}^2}} \exp\left(- \frac{\left(x - I_{1(0)}\right)^2}{2\sigma_{\mathrm{b}}^2} \right) \mathrm{d}h_{1(0)}^{a}\, \mathrm{d}x, \end{aligned} \tag{22}$$

$$\begin{aligned} &p_{\mathrm{ce}}(0|1,\, n) \\ &= \int_0^{\infty} \int_{-\infty}^{I_{\mathrm{D}}} f_{\mathrm{P}}\left(h_{1(1)}^{a}\right) \frac{1}{\sqrt{2\pi\sigma_{\mathrm{b}}^2}} \exp\left(- \frac{\left(x - I_{1(1)}\right)^2}{2\sigma_{\mathrm{b}}^2} \right) \mathrm{d}h_{1(1)}^{a}\, \mathrm{d}x, \end{aligned} \tag{23}$$

where I_{D} is the chip detection threshold, which is assumed to be fixed. $f_{\mathrm{P}}(h_{1(0)}^{a})$, $f_{\mathrm{P}}(h_{1(1)}^{a})$ correspond to the joint pdf of log-normal vector of length n and $n+1$, respectively. It is worth noting that $h_{1(0)} = h_1^{\mathrm{l}} h_1^{\mathrm{p}} h_{1(0)}^{a}$ and $h_{1(1)} = h_1^{\mathrm{l}} h_1^{\mathrm{p}} h_{1(1)}^{a}$, where h_1^{l} and h_1^{p} are the channel loss coefficient and the fraction of the collected power of the first hop, respectively.

Performing $z_0 = \ln(h_{1(0)}^{a})$ and $z_1 = \ln(h_{1(1)}^{a})$ transformations, we have

$$p_{\mathrm{ce}}(1|0,\, n) = \int_{-\infty}^{\infty} \Omega\left(z_0,\, \mu_{z_0},\, \sigma_{z_0}^2\right) Q\left(\frac{I_{\mathrm{D}} - \Re P_{\mathrm{c}} h_1^{\mathrm{l}} h_1^{\mathrm{p}} \exp(z_0)}{\sigma_{\mathrm{b}}} \right) \mathrm{d}z_0 \tag{24}$$

$$p_{\mathrm{ce}}(0|1,n)=\int_{-\infty}^{\infty}\Omega\left(z_1,\mu_{z_1},\sigma_{z_1}^2\right)Q\left(\frac{\Re P_{\mathrm{c}}h_1^{\mathrm{l}}h_1^{\mathrm{p}}\exp\left(z_1\right)-I_{\mathrm{D}}}{\sigma_{\mathrm{b}}}\right)\mathrm{d}z_1, \tag{25}$$

where $Q(u)=\int_u^{\infty}\Omega(x,0,1)\,\mathrm{d}x$. Furthermore, (24) and (25) can be approximated by Gauss-Hermite quadrature formula (shown in (38) in Appendix 2)

$$p_{\mathrm{ce}}(1|0,n)\simeq\sum_{t=1}^{v}\frac{g_t}{\sqrt{\pi}}Q\left(\frac{I_{\mathrm{D}}-\Re P_{\mathrm{c}}h_1^{\mathrm{l}}h_1^{\mathrm{p}}\exp\left(\mu_{z_0}+m_t\sigma_{z_0}\sqrt{2}\right)}{\sigma_{\mathrm{b}}}\right), \tag{26}$$

$$p_{ce}(0|1,n)\simeq\sum_{t=1}^{v}\frac{g_t}{\sqrt{\pi}}Q\left(\frac{\Re P_c h_1^l h_1^p\exp\left(\mu_{z_1}+m_t\sigma_{z_1}\sqrt{2}\right)-I_D}{\sigma_b}\right), \tag{27}$$

where m_t and g_t are the zero of the tth-order Hermite polynomial value and the weight factor for the tth-order approximation, respectively.

4.3 CEP for the mth hop (m = 2, 3, ..., N + 1)

For the m-hop with $m=2, 3, \ldots, N+1$, there is no additional MAI but still having the presence of atmospheric channel effects and background noise. Therefore, the received current at relay (R_i) can be expressed as

$$I_m=\begin{bmatrix}I_{m(0)}\\ I_{m(1)}\end{bmatrix}=\begin{bmatrix}n_{\mathrm{b}}\\ \Re P_{\mathrm{c}}h_m+n_{\mathrm{b}}\end{bmatrix}, \tag{28}$$

By following the mathematical transformations as presented in the previous subsection, we can derive the CEP for the mth hop as

$$p_{\mathrm{ce}-m}(1|0,k)=Q\left(\frac{I_{\mathrm{D}}}{\sigma_{\mathrm{b}}}\right), \tag{29}$$

$$p_{\mathrm{ce}-m}(0|1,k)\simeq\sum_{t=1}^{v}\frac{g_t}{\sqrt{\pi}}Q\left(\frac{\Re P_{\mathrm{c}}h_i^{\mathrm{l}}\exp\left(\mu_z+m_t\sigma_z\sqrt{2}\right)-I_{\mathrm{D}}}{\sigma_{\mathrm{b}}}\right). \tag{30}$$

4.4 End-to-end CEP

In relay-assisted AO/CDMA systems, there is a possibility that the receiver may still detect correctly a chip although that chip is detected incorrectly in an even number of times in the previous relays. For the worst-case performance, we consider that the end-to-end CEP is the probability that chips are transmitted without error between any pair of two consecutive relays, and it can be expressed as

$$p_{e2e}(1|0,k)=1-\prod_{m=1}^{N+1}\left(1-p_{\mathrm{ce}-m}(1|0,k)\right), \tag{31}$$

$$p_{e2e}(0|1,k)=1-\prod_{m=1}^{N+1}\left(1-p_{\mathrm{ce}-m}(0|1,k)\right). \tag{32}$$

5 Security analysis

To demodulate user's data, an eavesdropper has to detect exactly the code word of the user. By locating a receiver in the coverage of the optical beam, the eavesdropper is able to detect the coded transmissions of users to perform the necessary calculations and derive the code from this information. The resulting code will have some probability of error, which depends strongly on the signal-to-noise ratio at the eavesdropper's receiver.

Similar to [21], in our analysis, we consider the worst case assumption from a security perspective (i.e. the best possible performance for the eavesdropper) that the eavesdropper is able to synchronise the user's signal, locate the beginning and ending of a data bit, and then can sample the detector output precisely at the end of each code chip time. Code interception performance is calculated based on the average probability that the eavesdropper can detect the user's entire code word with no errors, denoted by P_{correct}. This probability, therefore, can be computed from the probability of missing a transmitted pulse in a given chip time (P_{M}) and the probability of falsely detecting a pulse in a chip time where none was transmitted (P_{F}) as

$$P_{\mathrm{correct}}=\sum_{k=1}^{K-1}\binom{K-1}{k}2^{1-K}(1-P_{\mathrm{M}})^{p_{\mathrm{s}}}(1-P_{\mathrm{F}})^{p_{\mathrm{s}}^2p_h-p_{\mathrm{s}}}, \tag{33}$$

where the first term represents the probability of not missing any of the pulses that are transmitted during a data bit; the second term is the probability of not falsely detecting pulses in any of the $p_{\mathrm{s}}^2p_h-p_{\mathrm{s}}$ chip time where pulses are not transmitted during a data bit.

Assuming that the eavesdropper places its receiver next to the node m (a relay or destination) to detect the coded transmissions. The distance between the eavesdropper's receiver and that of relays (or destination) is denoted as r (see Fig. 3), thus the fraction of power collected by the eavesdropper is $h_{\mathrm{p}}(\mathrm{r};z)$ where r is larger than zero. P_{M} and P_{F}, are the accumulated CEPs that the user transmits chip '1' but the eavesdropper detects chip '0' and the user transmits chip '0' but the eavesdropper detects chip '1', respectively. P_{M} and P_{F}, therefore, can be expressed as

$$P_{\mathrm{M}-m}=1-\prod_{j=1}^{m}\left(1-p_{\mathrm{ce}-j}(1|0,k)\right), \tag{34}$$

$$P_{\mathrm{F}-m}=1-\prod_{j=1}^{m}\left(1-p_{\mathrm{ce}-j}(0|1,k)\right). \tag{35}$$

6 Numerical results

This section presents numerical results of the proposed system BER and security analysis. We assume the distance of L km from the source to the destination and the consecutive nodes are equidistant along the path. The numerical results are considered under a constraint on the fixed energy per bit E_{b}. Because there are p_{s} pulses in one bit duration, which are assumed to have equal power, the relation between the energy per bit and the power per chip is given by $P_{\mathrm{c}}=(E_{\mathrm{b}}/p_{\mathrm{s}})/T_{\mathrm{c}}$, where $(E_{\mathrm{b}}/p_{\mathrm{s}})$ and T_{c} are the chip energy and chip duration, respectively. In addition, the threshold detection level I_{D} can be calculated as $I_{\mathrm{D}}=\Re P_{\mathrm{c}}h^{\mathrm{l}}D$, where D is the normalised threshold and set at the same level for all hops along the transmission path. The effective electrical bandwidth, B_{e}, is fixed at 70% of the chip rate [16]. The relation between the chip rate R_{c} and the bit rate per user (R_{b}) can be expressed as $R_{\mathrm{c}}=R_{\mathrm{b}}p_{\mathrm{s}}^2$, where (p_{s}^2) is the code length. Other system parameters and constants used in the analysis are shown in Table 2.

6.1 BER performance

The BER of 10^{-9} is the error probability at which the communication systems can be considered as error-free. In our analysis, BER of 10^{-6} is targeted so that, under the assumption that FEC is used used, the error-free communications can be guaranteed.

First, Fig. 4 investigates the system BER against the normalised threshold with the number of relays varies from 1 to 3. To achieve low BER, the normalised threshold should be chosen properly. If D is too small, system's performance is degraded due to detecting

Table 2 System parameters and constants

Name	Symbol	Value
electron charge	e	1.602×10^{-19} C
PD responsivity	$\Re$	0.6 A/W
attenuation coefficient	β	1 km^{-1}
receiver diameter	$2a$	20 cm
beam radius at 1 km	ω_z	2.5 m
background power	P_b	−30 dBm
wavelength	λ	1550 nm
refractive index structure coeff.	C_n^2	10^{-15} m$^{-2/3}$

chip '1' when none was transmitted. In the case when D is too large, error detection is induced by falsely detecting chip '0' when chip '1' was transmitted. The optimum threshold selection depends on parameter settings, especially the number of relays. When the number of relays is large enough, BER reaches the floor and the selection of threshold can be chosen from a wide range of values.

In Fig. 5, the relation between the BER and the number of active users K is investigated with different code sets, that is, different values of p_s and p_h. This figure is obtained based on the optimum threshold selection shown in Fig. 4. It is clearly seen that BER is reduced by increasing either p_s or p_h. When p_s is increased, BER is improved more significantly. Moreover, the number of supportable users at a specific value of BER can be determined from this result. As shown in the figure, the system using $p_s = 7$ and $p_h = 7$ (i.e. 7 wavelengths) can support 15 users with the BER of 10^{-6}, which is above twice times the required number of wavelengths. This is an advantage of AO systems using CDMA compared with the ones using wavelength-division multiple-access.

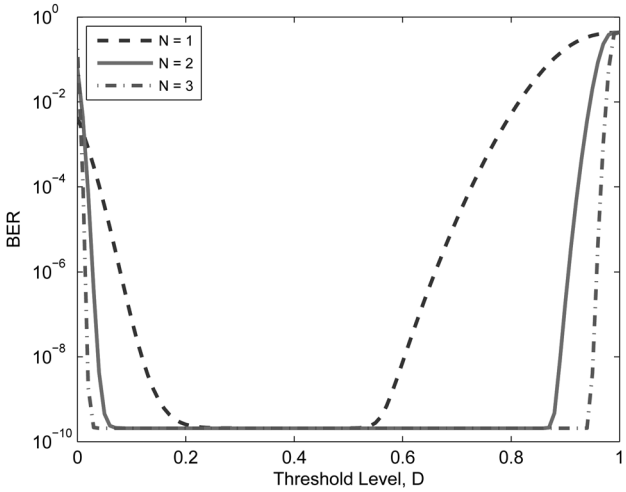

Fig. 4 *BER against the normalised threshold (D) with $E_b = -130$ dBJ, $R_b = 5$ Gbps, $L = 3$ km, $K = 4$ users, and $\{p_s;p_h\} = \{7;7\}$*

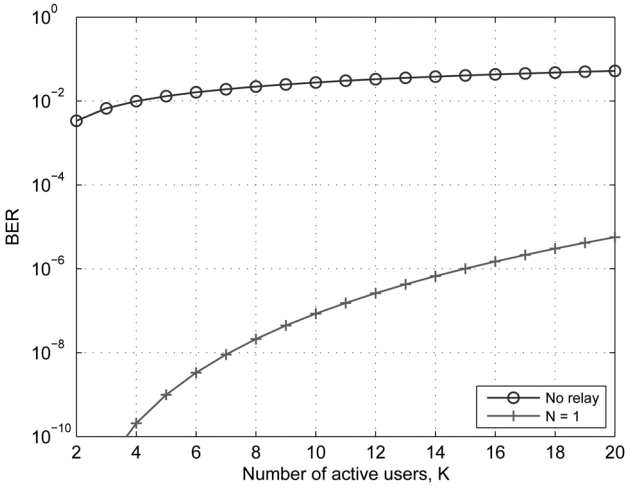

Fig. 6 *BER against the number of active users (K) with $E_b = -130$ dBJ, $R_b = 5$ Gbps, $L = 3$ km, and $\{p_s;p_h\} = \{7;7\}$*

The benefits of using relay transmission are quantified in Fig. 6, which also shows BER versus the number of active users K. Under the impacts of physical layer impairments, including atmospheric turbulence, MAI, and background noise, BER of AO/CDMA systems without relaying is very high even when the number of users is small. On the other hand, the use of relay transmission can help to reduce BER significantly. As a result, the relay-assisted AO/CDMA systems with one relays can support more than 10 users with BER of 10^{-6} when $L = 3$ km and $R_b = 1$ Gbps.

To further examine the gain of using relay transmission in terms of transmission distance, Fig. 7 demonstrates the BER as a function of L with $E_b = -130$ dBJ. In this case, BER floor is governed by the number of active users that is related to the strength of MAI. It is seen that the transmission distance that AO/CDMA systems can support (at a specific BER) increases with the number of relays. For example, at $K = 4$ users and BER of 10^{-6}, the transmission distance increases from 3.5 to 5.2 km when the number of relays

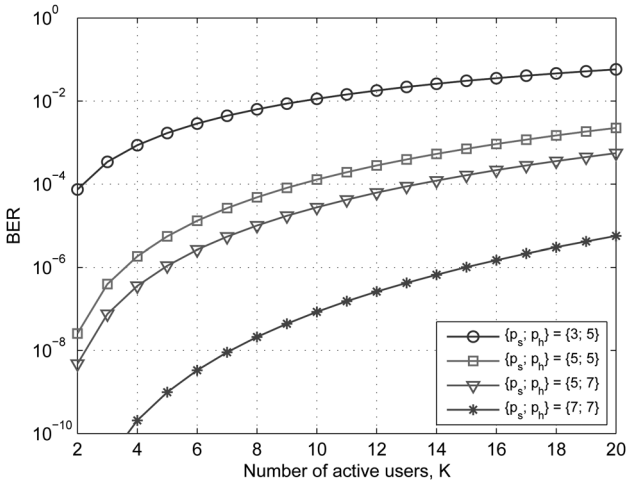

Fig. 5 *BER against the number of active users (K) with $E_b = -130$ dBJ, $R_b = 5$ Gbps, $L = 3$ km, and $N = 2$*

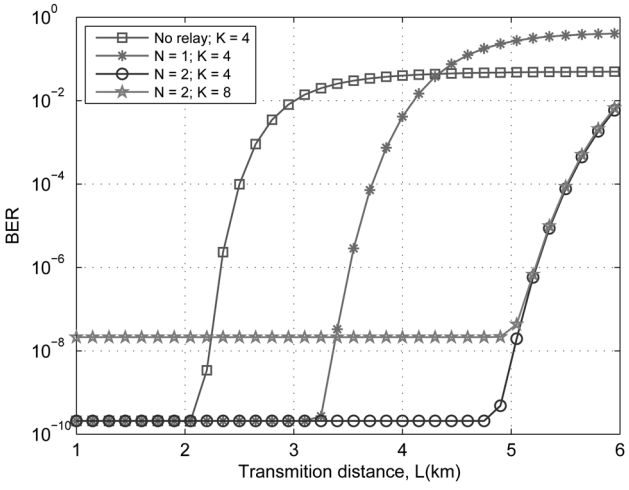

Fig. 7 *BER against the transmission distance with $E_b = -130$ dBJ, $R_b = 5$ Gbps, and $\{p_s;p_h\} = \{7;7\}$*

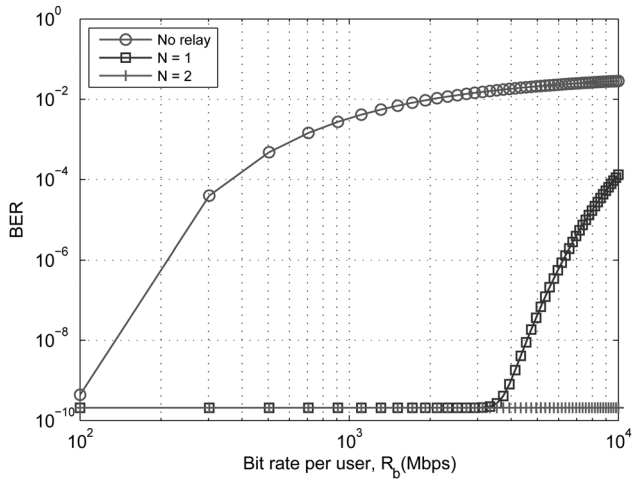

Fig. 8 *BER against the bit rate per user with average bit power of −5 dBm, L = 4 km, K = 4 users and {p_s;p_h} = {7;7}*

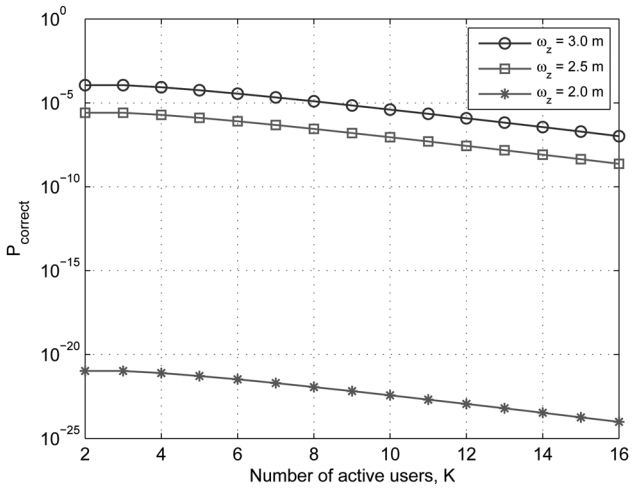

Fig. 10 *$P_{correct}$ against the number of active user K with $E_b = -130$ dBJ, $R_b = 5$ Gbps, L = 5 km, N = 3, r = 3 m, and {p_s;p_h} = {7;7}*

increases from 1 to 2. Obviously, longer transmission distance can be achieved by deploying more relays.

System BER is investigated versus the bit rate per user in Fig. 8 under a constraint of fixed power per bit, that is, E_bR_b is a constant and set to be -5 dBm. The transmission distance $L = 3$ km and the number of users $K = 4$. Similar to the previous results, BER floor is governed by the number of active users. In the case of no relay, the supportable bit rate per user with BER of 10^{-9} is below 200 Mbps. By increasing the number of relays, the supportable bit rate per user can be increased. In particular, the bit rate per user of 4 Gbps (also at BER of 10^{-9}) can be supported with one relay. In the case of using two relays, BER reaches the floor for any bit rate from 100 Mbps to 10 Gbps.

6.2 Security performance

Fig. 9 depicts the average probability that the eavesdropper can detect the user's entire code word with no errors P_{correct} against the transmitted power per bit P_s. Several values of r, the distance between the targeted receiver and the eavesdropper's receiver, are investigated in the figure. The increase of transmitted power helps to reduce BER, however it causes the decrease of confidentiality, that is, P_{correct} increases. Confidentiality is also decreased when the eavesdropper's receiver is located near the targeted receiver. This is because the fraction of optical power that reaches unauthorised receiver increases with r as shown in (6).

Finally, we investigate P_{correct} as a function of the number of active users K in Fig. 10. Thanks to the effect of MAI from interfering users, P_{correct} is reduced when K increases. In addition, confidentiality can be increased by reducing the width of the optical beam. Although a FSO system with narrow beam is considerably affected by pointing error, an auto-tracking scheme may overcome this problem.

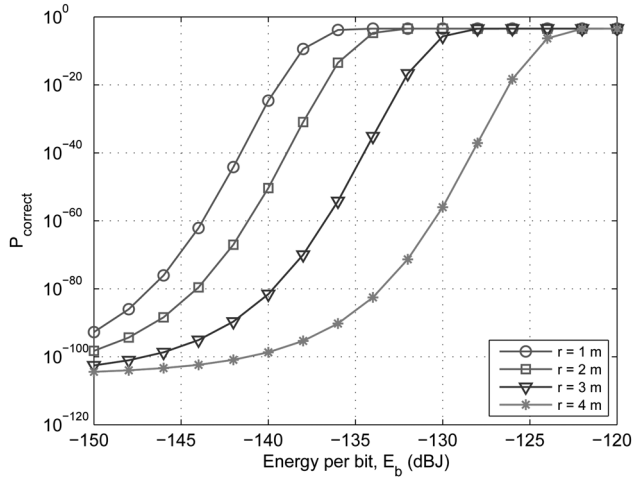

Fig. 9 *$P_{correct}$ against total transmitted power per bit $E_b = -130$ dBJ with K = 4 users, $R_b = 5$ Gbps, L = 5 km, N = 3, and {p_s;p_h} = {7;7}*

7 Conclusion

We have presented the method to formulate the mathematical expression for BER of relay-assisted AO/CDMA systems over log-normal turbulence channel. Other physical layer impairments were also taken into consideration including atmospheric attenuation, beam spreading, MAI, and background noise. The numerical results showed that relay transmission helps to significantly reduce the effect of atmospheric turbulence, hence AO/CDMA system could achieve a large number of users and long transmission distance. The security performance of the proposed system was also investigated with several values of system parameters including the location of eavesdropper and the beam width. High confidentiality could be achieved by properly selecting the system parameters. Thanks to the above-mentioned advantages, serial relaying of the AO/CDMA systems could be a promising candidate for the next generation broadband access networks.

8 Acknowledgment

This research was funded by Vietnam National Foundation for Science and Technology Development (NAFOSTED) under grant no. 102.02-2013.02.

9 References

1 Heatley, D.J., Wisely, D.R., Neild, I., Cochrane, P.: 'Optical wireless: the story so far', *IEEE Commun. Mag.*, 1998, **36**, (12), pp. 72–82
2 Liu, Q., Qiao, C., Mitchell, G., Stanton, S.: 'Optical wireless communication networks for first- and last-mile broadband access [Invited]', *J. Opt. Netw.*, 2005, **4**, (12), pp. 807–828
3 Ohtsuki, T.: 'Performance analysis of atmospheric optical PPM CDMA systems', *J. Lightwave Technol.*, 2005, **21**, (2), pp. 406–411
4 Ohba, K., Hirano, T., Miyazawa, T., Sasase, I.: 'A symbol detection scheme to mitigate effects of scintilations and MAIs in optical atmospheric PPM-CDMA systems'. Proc. IEEE Globecom, St. Louis, MO, November/December 2005, pp. 1999–2003

5 Jazayerifar, M., Salehi, J.A.: 'Atmospheric optical CDMA communications via optical orthogonal codes', *IEEE Trans. Commun.*, 2006, **54**, (9), pp. 1614–1623
6 Miyazawa, T., Sasase, I.: 'BER performance analysis of spectral phase-encoded optical atmospheric PPM-CDMA communication systems', *J. Lightwave Technol.*, 2007, **25**, (10), pp. 2992–3000
7 Pham, A.T., Luu, T.A., Dang, N.T.: 'Performance bound for turbo-coded 2-D FSO/CDMA systems over atmospheric turbulence channel', *IEICE Trans. Fundam.*, 2010, **93-A**, (12), pp. 2696–2699
8 Dang, N.T., Pham, A.T.: 'Performance improvement of FSO/CDMA systems over dispersive turbulence channel using multi-wavelength PPM signaling', *OSA Opt. Exp.*, 2012, **20**, (24), pp. 26786–26797
9 Zhu, X., Khan, J.M.: 'Free-space optical communication through atmospheric turbulence channels', *IEEE Trans. Commun.*, 2002, **50**, (8), pp. 1293–1300
10 Akella, J., Yuksel, M., Kalyanaraman, S.: 'Error analysis of multi-hop free-space optical communication'. Proc. of IEEE Int. Conf. on Communication, 2005, pp. 1777–1781
11 Safari, M., Uysal, M.: 'Relay-assisted free-space optical communication', *IEEE Trans. Wirel. Commun.*, 2008, **7**, (12), pp. 5441–5449
12 Datsikas, C.K., Peppas, K.P., Sagias, N.C., Tombras, G.S.: 'Serial free-space optical relaying communications over Gamma-Gamma atmospheric turbulence channels', *J. Opt. Commun. Netw.*, 2010, **2**, (8), pp. 576–586
13 Feng, M., Wang, J.B., Sheng, M., Cao, L.L., Xie, X.X., Chen, M.: 'Outage performance for parallel relay-assisted free-space optical communications in strong turbulence with pointing errors'. Proc. of International Conf. on Wireless Commun. and Signal Processing (WCSP), 2011, pp. 1–5
14 Chatzidiamantis, N.D., Michalopoulos, D.S., Kriezis, E.E., Karagiannidis, G.K., Schober, R.: 'Relay selection protocols for relay-assisted free-space optical systems', *IEEE/OSA J. Opt Commun. Netw.*, 2013, **5**, (1), pp. 92–103
15 Kashani, M., Safari, M., Uysal, M.: 'Optimal relay placement in cooperative free-space optical communication systems', *IEEE J. Opt. Commun. Netw.*, 2013, **5**, (1), pp. 37–47
16 Meenakshi, M., Andonovic, I.: 'Effect of physical layer impairments on SUM and AND detection strategies for 2-D optical CDMA', *IEEE Photon. Technol. Lett.*, 2005, **17**, (5), pp. 1112–1114
17 Tancevski, L., Andonovic, I.: 'Hybrid wavelength hopping/time spreading schemes for use in massive optical networks with increased security', *J. Lightw. Technol.*, 1996, **14**, (12), pp. 2636–2647
18 Ricklin, J.C., Davidson, F.M.: 'Atmospheric turbulence effects on a partially coherent Gaussian beam: implications for free space laser communication', *J. Opt. Soc. Amer. A, Opt. Image Sci.*, 2002, **19**, (9), pp. 1794–1802
19 Farid, A.A., Hranilovic, S.: 'Outage capacity optimization for free-space optical links with pointing errors', *IEEE J. Lightw. Technol.*, 2007, **25**, (7), pp. 1702–1710
20 Navidpour, S.M., Uysal, M., Kavehrad, M.: 'BER performance of free-space optical transmission with spatial diversity', *IEEE Trans. Wirel. Comm.*, 2007, **6**, (8), pp. 2813–2819
21 Shake, T.H.: 'Security performance of optical CDMA against eavesdropping', *IEEE J. Lightw. Technol.*, 2005, **23**, (2), pp. 655–670
22 Simon, M.K., Alouini, M.S.: 'Digital communication over fading channels' (John Wiley and Sons, New York, 2000)

10 Appendix 1: approximation for a sum of correlated log-normal random variables

This appendix shows an approach of approximation for the summation of correlated log-normal random variables. Particularly, we can approximate $\sum_{k=1}^{K} \exp(x_k)$, where pdf of all x_k are $\Omega(x_k, -\sigma_x^2/2, \sigma_x^2)$, to single log-normal variable $Z = \exp(z)$ with pdf of z is $\Omega(z, \mu_z, \sigma_z^2)$. We can have the closed-form of mean and variance of random variable z as given by [20]

$$\mu_z = \log(K) - \frac{\sigma_z^2}{2} \quad \text{and} \quad \sigma_z^2 \simeq \frac{1}{K}\sigma_x^2 + \frac{1}{K^2}\sum_{k \neq l} v_{kl}, \tag{36}$$

where $v_{kl} = \text{cov}(x_k, x_l)$ are cross-correlation values between x_k and x_l, $k \neq l$.

11 Appendix 2: Gauss–Hermite quadrature

Gauss–Hermite quadrature is a form of Gaussian quadrature used for approximating the value of an integral. If we have a Gaussian integral as

$$\int_{-\infty}^{\infty} \mathrm{e}^{-x^2} f(x)\,\mathrm{d}x, \tag{37}$$

then it can be approximated as [22]

$$\int_{-\infty}^{\infty} \mathrm{e}^{-x^2} f(x)\,\mathrm{d}x \simeq \sum_{i=1}^{n} w_i f(x_i), \tag{38}$$

where n is the required approximation order. x_i, $i = 1, 2, \ldots, n$ are zeros of the Hermite polynomial $H_n(x)$ and w_i, $i = 1, 2, \ldots, n$ are the associated weight factors which is given by [22]

$$w_i = \frac{2^{n-1} n! \sqrt{\pi}}{n^2 \left[H_{n-1}(x_i)\right]^2}. \tag{39}$$